Chapter 2
CIECAM02 and Its Recent Developments

Ming Ronnier Luo and Changjun Li

The reflection is for the colors what the echo is for the sounds

Joseph Joubert

Abstract The development of colorimetry can be divided into three stages: colour specification, colour difference evaluation and colour appearance modelling. Stage 1 considers the communication of colour information by numbers. The second stage is colour difference evaluation. While the CIE system has been successfully applied for over 80 years, it can only be used under quite limited viewing conditions, e.g., daylight illuminant, high luminance level, and some standardised viewing/illuminating geometries. However, with recent demands on crossmedia colour reproduction, e.g., to match the appearance of a colour or an image on a display to that on hard copy paper, conventional colorimetry is becoming insufficient. It requires a colour appearance model capable of predicting colour appearance across a wide range of viewing conditions so that colour appearance modelling becomes the third stage of colorimetry. Some call this as advanced colorimetry. This chapter will focused on the recent developments based on CIECAM02.

Keywords Color appearance model • CAM • CIECAM02 • Chromatic adaptation transforms • CAT • Colour appearance attributes • Visual phenomena • Uniform colour spaces

M.R. Luo (✉)
Zheijiang University, Hangzhou, China
University of Leeds, Leeds, UK
e-mail: M.R.Luo@Leeds.ac.uk

C. Li
Liaoning University of Science and Technology, Anshan, China

2.1 Introduction

The development of colorimetry [1] can be divided into three stages: colour specification, colour difference evaluation and colour appearance modelling. Stage 1 considers the communication of colour information by numbers. The Commission Internationale de l'Eclairage (CIE) recommended a colour specification system in 1931 and later, it was further extended in 1964 [2]. The major components include standard colorimetric observers, or colour matching functions, standard illuminants and standard viewing and illuminating geometry. The typical colorimetric measures are the tristimulus value (X, Y, Z), chromaticity coordinates (x, y), dominant wavelength, and excitation purity.

The second stage is colour difference evaluation. After the recommendation of the CIE specification system in 1931, it was quickly realised that the colour space based on chromaticity coordinates was far from a uniform space, i.e., two pairs of stimuli having similar perceived colour difference would show large difference of the two distances from the chromaticity diagram. Hence, various uniform colour spaces and colour difference formulae were developed. In 1976, the CIE recommended CIELAB and CIELUV colour spaces [2] for presenting colour relationships and calculating colour differences, More recently, the CIE recommended the CIEDE2000 [3] for evaluating colour differences.

While the CIE system has been successfully applied for over 80 years, it can only be used under quite limited viewing conditions, for example, daylight illuminant, high luminance level, and some standardised viewing/illuminating geometries. However, with recent demands on cross-media colour reproduction, for example, to match the appearance of a colour or an image on a display to that on hard copy paper, conventional colorimetry is becoming insufficient. It requires a colour appearance model capable of predicting colour appearance across a wide range of viewing conditions so that colour appearance modelling becomes the third stage of colorimetry. Some call this as advanced colorimetry.

A great deal of research has been carried out to understand colour appearance phenomena and to model colour appearance. In 1997, the CIE recommended a colour appearance model designated CIECAM97s [4,5], in which the "s" represents a simple version and the "97" means the model was considered as an interim model with the expectation that it would be revised as more data and better theoretical understanding became available. Since then, the model has been extensively evaluated by not only academic researchers but also industrial engineers in the imaging and graphic arts industries. Some shortcomings were identified and the original model was revised. In 2002, a new model: CIECAM02 [6, 7] was recommended, which is simpler and has a better accuracy than CIECAM97s.

The authors previously wrote an article to describe the developments of CIECAM97s and CIECAM02 [8]. The present article will be more focused on the recent developments based on CIECAM02. There are six sections in this chapter. Section 2.2 defines the viewing conditions and colour appearance terms used in CIECAM02. Section 2.3 introduces some important colour appearance data

sets which were used for deriving CIECAM02. In Sect. 2.4, a brief introduction of different chromatic adaptation transforms (CAT) leading to the CAT02 [8], embedded in CIECAM02, will be given. Section 2.5 gives various visual phenomena predicted by CIECAM02. Section 2.6 summarises some recent developments of the CIECAM02. For example, the new uniform colour spaces based on CIECAM02 by Luo et al. (CAM02-UCS, CAM02-SCD and CAM02-LCD) [9] will be covered. Xiao et al. [10–12] extended CIECAM02 to predict the change in size of viewing field on colour appearance, known as size effect. Fu et al. [13] has extended the CIECAM02 for predicting colour appearances of unrelated colours presented in mesopic region. Finally, efforts were paid to modify the CIECAM02 in connection with international color consortium (ICC) profile connection space for the colour management [14]. In the final section, the authors point out a concept of the universal model based on CIECAM02.

2.2   Viewing Conditions and Colour Appearance Attributes

The step-by-step calculation of CIECAM02 is given in Appendix. In order to use CIECAM02 correctly, it is important to understand the input and output parameters of the model. Figure 2.1 shows the viewing parameters, which define the viewing conditions, and colour appearance terms, which are predicted by the model. Each of them will be explained in this section. X_w, Y_w, Z_w are the tristimulus values of the reference white under the test illuminant; L_A specifies the luminance of the adapting field; Y_b defines the luminance factor of background; the definition of surround will be introduced in later this section.

The output parameters from the model include Lightness (J), Brightness (Q), Redness–Greenness (a), Yellowness–Blueness (b), Colourfulness (M), Chroma (C), Saturation (s), Hue composition (H), and Hue angle (h). These attributes will also be defined in this section.
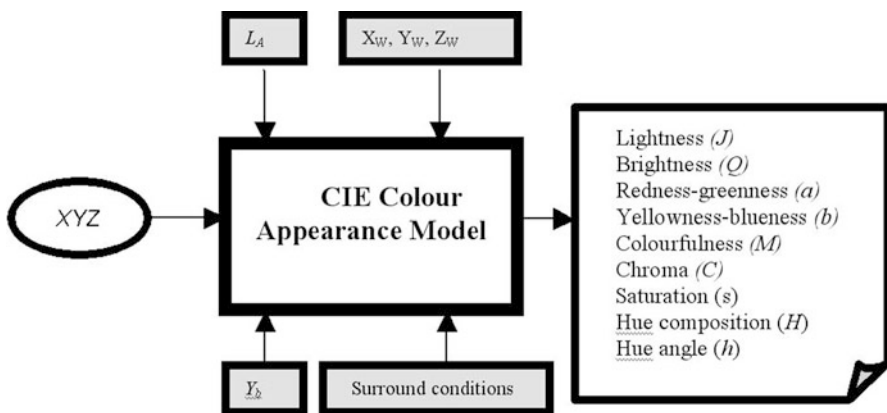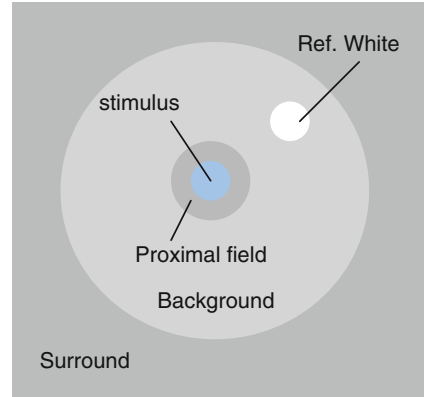

Fig. 2.1 A schematic diagram of a CIE colour appearance model

Fig. 2.2 Configuration for
viewing colour patches of
related colours

2.2.1 Viewing Conditions

The aim of the colour appearance model is to predict the colour appearance under
different viewing conditions. Various components in a viewing field have an impact
on the colour appearance of a stimulus. Hence, the accurate definition of each
component of the viewing field is important. Figures 2.2–2.4 are three configurations
considered in this chapter: colour patches for related colours, images for related
colours, and patches for unrelated colours. The components in each configuration
will be described below. Note that in the real world, objects are normally viewed
in a complex context of many stimuli; they are known as "related" colours. An
"unrelated colour" is perceived by itself, and is isolated, either completely or
partially, from any other colours. Typical examples of unrelated colours are signal
lights, traffic lights, and street lights, viewed in a dark night.

2.2.1.1 Stimulus

In Figs. 2.2 and 2.4 configurations, the stimulus is a colour element for which a
measure of colour appearance is required. Typically, the stimulus is taken to be
a uniform patch of about $2°$ angular subtense. A stimulus is first defined by the
tristimulus values (X, Y, Z) measured by a tele-spectroradiometer (TSR) and then
normalised against those of reference white so that Y is the percentage reflection
factor.

In Fig. 2.3 configuration, the stimulus becomes an image. The pixel of each
image is defined by device independent coordinates such as CIE XYZ or CIELAB
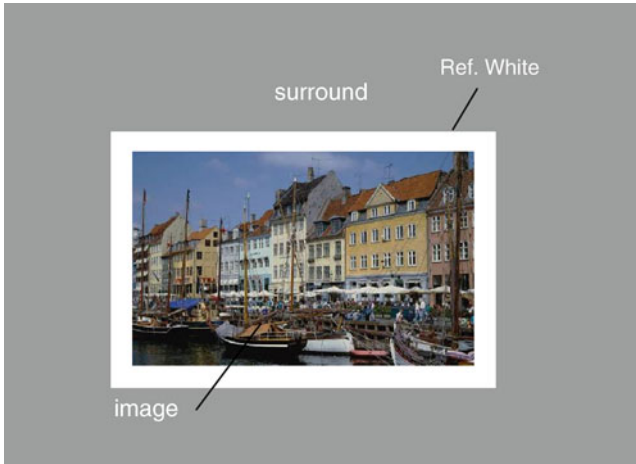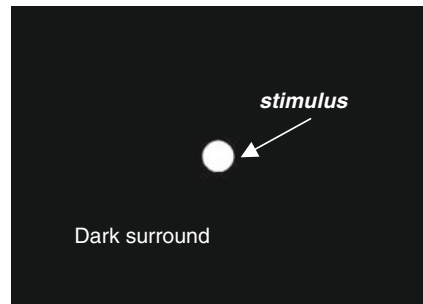values.

Fig. 2.3 Configuration for viewing images

Fig. 2.4 Configuration for viewing unrelated colours

2.2.1.2 Proximal Field

In Fig. 2.2 configuration, proximal field is the immediate environment of the colour element considered, extending typically for about 2° from the edge of that colour element in all or most directions. Currently, proximal field is not used in CIECAM02. It will be applied when simultaneous contrast effect to be introduced in the future.

This element is not considered in Figs. 2.3 and 2.4 configurations.

2.2.1.3 Reference White

In Fig. 2.2 configuration, the reference white is used for scaling lightness (see later) of the test stimulus. It is assigned to have a lightness of 100. It is measured by a TSR again to define the tristimulus values of the light source (X_W, Y_W, Z_W) in cd/m^2 unit. The parameter of L_W (equal to Y_W) in the model defines the luminance of the

light source. When viewing unrelated colours, there is no such element. For viewing images, the reference white will be the white border (about 10 mm) surrounding the image.

The reference white in this context can be considered as the "adopted white" i.e., the measurement of "a stimulus that an observer who is adapted to the viewing environment would judge to be perfectly achromatic and to have a reflectance factor of unity (i.e., have absolute colorimetric coordinates that an observer would consider to be the perfect white diffuser)" [ISO 12231] For viewing an image, there could be some bright areas such as a light source or specularly reflecting white objects, possibly illuminated by different sources. In the latter case, the "adopted white" (the actual stimulus which an observer adapted to the scene judges to be equivalent to a perfect white diffuser) may be different from the adopted white measured as above.

2.2.1.4 Background

In Fig. 2.2 configuration, background is defined as the environment of the colour element considered, extending typically for about $10°$ from the edge of the proximal field in all, or most directions. When the proximal field is the same colour as the background, the latter is regarded as extending from the edge of the colour element considered. Background is measured by a TSR to define background luminance, L_b. In CIECAM02, background is defined by the luminous factor, $Y_b = 100 \times L_b/L_W$.

There is no such element for Fig. 2.4 configuration, normally in complete darkness. For viewing images (Fig. 2.3), this element can be the average Y value for the pixels in the entire image, or frequently, a Y value of 20, approximate an L* of 50 is used.

2.2.1.5 Surround

A surround is a field outside the background in Fig. 2.2 configuration, and outside the white border (reference white) in Fig. 2.3. Surround includes the entire room or the environment. Figure 2.4 configuration has a surround in complete darkness.

Surround is not measured directly, rather the surround ratio is determined and used to assign a surround. The surround ratio, S_R, can be computed:

$$S_R = L_{SW}/L_{DW}, \qquad (2.1)$$

where L_{SW} is the luminance of the surround white and L_{DW} is the luminance of the device white. L_{SW} is a measurement of a reference white in the surround field while L_{DW} is a measurement of the device white point for a given device, paper or peak white. If SR is 0, then a dark surround is appropriate. If S_R is less than 0.2, then a dim surround should be used while an S_R of greater than or equal to 0.2 corresponds to an average surround. Different surround "average," "dim," "dark" leads to different

Table 2.1 Parameter settings for some typical applications

Example	Ambient illumination in lux (or cd/m^2)	Scene or device white luminance	L_A in cd/m^2	Adopted white point	S_R	Surround
Surface colour evaluation in a light booth	1,000 (318.3)	318.30 cd/m^2	60	Light booth	1	Average
Viewing self-luminous display at home	38 (12)	80 cd/m^2	20	Display and ambient	0.15	Dim
Viewing slides in dark room	0 (0)	150 cd/m^2	30	Projector	0	Dark
Viewing self-luminous display under office illumination	500 (159.2)	80 cd/m^2	15	Display	2	Average

parameters (F: incomplete adaptation factor; Nc: chromatic induction factor and c: impact of surround) used in CIECAM02. Table 2.1 define S_R values in some typical examples in real applications.

2.2.1.6   Adapting Field

For Fig. 2.2 configuration, adapting field is the total environment of the colour element considered, including the proximal field, the background and the surround, and extending to the limit of vision in all directions. For Fig. 2.3 image configuration, it can be approximated the same as background, i.e., approximate an L* of 50.

The luminance of adapting field is expressed as L_A, which can be approximated by $L_W \times Y_b/100$, or by L_b.

Photopic, Mesopic and Scotopic Vision

Another parameter is also very important concerning the range of illumination from the source. It is well known that rods and cones in our eyes are not uniformly distributed on the retina. Inside the foveola (the central 1° field of the eye), there are only cones; outside, there are both cones and rods; in the area beyond about 40° from the visual axis, there are nearly all rods and very few cones. The rods provide monochromatic vision under low luminance levels; this scotopic vision is in operation when only rods are active, and this occurs when the luminance level is less than about 0.1 cd/m^2. Between this level and about 10 cd/m^2, vision involves a mixture of rod and cone activities, which is referred to as mesopic vision. It requires luminance of about 10 cd/m^2 for photopic vision in which only cones are active.

2.2.2 Colour Appearance Attributes

CIECAM02 predicts a range of colour appearance attributes. For each attribute, it will be accurately defined mainly following the definitions of CIE International Lighting Vocabulary [15]. Examples will be given to apply them in the real-world situation, and finally the relationship between different attributes will be introduced.

2.2.2.1 Brightness (Q)

This is a visual perception according to which an area appears to exhibit more or less light. This is an openended scale with a zero origin defining the black.

The brightness of a sample is affected by the luminance of the light source used. A surface colour illuminated by a higher luminance would appear brighter than the same surface illuminated by a lower luminance. This is known as "Steven Effect" (see later).

Brightness is an absolute quantity, for example, a colour appears much brighter when it is viewed under bright outdoor sunlight than under moonlight. Hence, their Q values could be largely different.

2.2.2.2 Lightness (J)

This is the brightness of an area judged relative to the brightness of a similarly illuminated reference white.

It is a relative quantity, for example, thinking a saturated red colour printed onto a paper. The paper is defined as reference white having a lightness of 100. By comparing the light reflected from both surfaces in the bright sunlight, the red has a lightness of about 40% of the reference white (J value of 40). When assessing the lightness of the same red colour under the moonlight against the same reference white paper, the lightness remains more or less the same with a J of 40.

It can be expressed by $J = Q_S/Q_W$, where Q_S and Q_W are the brightness values for the sample and reference white, respectively.

2.2.2.3 Colourfulness (M)

Colourfulness is that attribute of a visual sensation according to which an area appears to exhibit more or less chromatic content.

This is an open-ended scale with a zero origin defining the neutral colours. Similar to the brightness attribute, the colourfulness of a sample is also affected by luminance. An object illuminated under bright sunlight would appear more colourful than when viewed under moonlight, such as M value changes from 2000 to 1 with a ratio of 2000.

Fig. 2.5 An image to illustrate saturation

2.2.2.4   Chroma (C)

This is the colourfulness of an area judged as a proportion of the brightness of a similarly illuminated reference white. This is an open-ended scale with a zero origin representing neutral colours. It can be expressed by $C = M/Q_W$.

The same example is given here, a saturated red printed on a white paper. It has a colourfulness of 50 against the white paper having a brightness of 250 when viewed under sunlight. When viewed under dim light, colourfulness reduces to 25 and brightness of paper also reduces to half. Hence, the C value remains unchanged.

2.2.2.5   Saturation (S)

This is the colourfulness of an area judged in proportion to its brightness as expressed by $s = M/Q$, or $s = C/J$. This scale runs from zero, representing neutral colours, with an open end.

Taking Figs. 2.3–2.5 as an example, the green grass under sunlight is bright and colourful. In contrast, those under the tree appear dark and less colourful. Because they are the same grass in the field, we know that they have the same colour, but their brightness and colourfulness values are largely different. However, their saturation values will be very close because it is the ratio between brightness and colourfulness. Similar example can also be found in the image on the brick wall. Hence, saturation could be a good measure for detecting the number and size of objects in an image.

2.2.2.6   Hue (H and H)

Hue is the attribute of a visual sensation according to which an area appears to be similar to one, or to proportions of two, of the perceived colours red, yellow, green and blue.

CIECAM02 predicts hue with two measures: hue angle (h) ranging from $0°$ to $360°$, and hue composition (H) ranging from 0, through 100, 200, 300, to 400 corresponding to the psychological hues of red, yellow, green, blue and back to red. These four hues are the psychological hues, which cannot be described in terms of any combinations of the other colour names. All other hues can be described as a mixture of them. For example, an orange colour should be described as mixtures of red and yellow, such as 60% of red and 40% of yellow.

2.3   Colour Appearance Data Sets

Colour appearance models based on colour vision theories have been developed to fit various experimental data sets, which were carefully generated to study particular colour appearance phenomena. Over the years, a number of experimental data sets were accumulated to test and develop various colour appearance models. Data sets investigated by CIE TC 1-52 CAT include: Mori et al. [16] from the Color Science Association of Japan, McCann et al. [17] and Breneman [18] using a haploscopic matching technique; Helson et al. [19], Lam and Rigg [20] and Braun and Fairchild [21] using the memory matching technique; and Luo et al. [22, 23] and Kuo and Luo [24] using the magnitude estimation method. These data sets, however, do not include visual saturation correlates. Hence, Juan and Luo [25, 26] investigated a data set of saturation correlates using the magnitude estimation method. The data accumulated played an important role in the evaluation of the performance of different colour appearance models and the development of the CIECAM97s and CIECAM02.

2.4   Chromatic Adaptation Transforms

Arguably, the most important function of a colour appearance model is chromatic adaptation transform. CAT02 is the chromatic adaptation transformation imbedded in CIEAM02. This section covers the developments towards this transform.

Chromatic adaptation has long been extensively studied. A CAT is capable of predicting corresponding colours, which are defined as pairs of colours that look alike when one is viewed under one illuminant (e.g., D65[1]) and the other is under

---

[1]In this chapter we will use for simplified terms "D65" and "A" instead of the complete official CIE terms: "CIE standard illuminant D65" and "CIE standard illuminant A".

a different illuminant (e.g., A). The following is divided into two parts: light and chromatic adaptation, and the historical developments of Bradford transform [20], CMCCAT2000 [27] and CAT02.

2.4.1 Light and Chromatic Adaptation

Adaptation can be divided into two: light and chromatic. The former is the adaptation due to the change of light levels. It can be further divided into two: light adaptation and dark adaptation. Light adaptation is the decrease in visual sensitivity upon an increase in the overall level of illumination. An example occurs when entering a bright room from a dark cinema. Dark adaptation is opposite to light adaptation and occurs, for example, when entering a dark cinema from a well-lit room.

2.4.2 Physiological Mechanisms

The physiology associated with adaptation mainly includes rod–cone transition, pupil size (dilation and constriction), receptor gain and offset. As mentioned earlier, the two receptors (cones and rods) functioning entirely for photopic (above approximately 10 cd/m^2) and for scotopic (below approximately 0.01 cd/m^2), respectively. Also, both are functioning in mesopic range between the two (approximately from 0.01 cd/m^2 to 10 cd/m^2).

The pupil size plays an important role in adjusting the amount of light that enters the eye by dilating or constricting the pupil: it is able to adjust the light by a maximum factor of 5. During dark viewing conditions, the pupil size is the largest. Each of the three cones responds to light in a nonlinear manner and is controlled by the gain and inhibitory mechanisms.

Light and dark adaptations only consider the change of light level, not the difference of colour between two light sources (up to the question of Purkinje shift due to the difference in the spectral sensitivity of the rods and cones). Under photopic adaptation conditions, the difference between the colours of two light sources produces chromatic adaptation. This is responsible for the colour appearance of objects, and leads to the effect known as colour constancy (see also Chap. 2: Chromatic constancy). The effect can also be divided into two stages: a "chromatic shift" and an "adaptive shift". Consider, for example, what happens when entering a room lit by tungsten light from outdoor daylight. We experience that all colours in the room instantly become reddish reflecting the relative hue of the tungsten source. This is known as the "colorimetric shift" and it is due to the operation of the sensory mechanisms of colour vision, which occur because of the changes in the spectral power distribution of the light sources in question. After a certain short adaptation period, the colour appearances of the objects become more

normal. This is caused by the fact that most of coloured objects in the real world are more or less colour constant (they do not change their colour appearance under different illuminants). The most obvious example is white paper always appears white regardless of which illuminant it is viewed under. The second stage is called the "adaptive shift" and it is caused by physiological changes and by a cognitive mechanism, which is based upon an observer's knowledge of the colours in the scene content in the viewing field. Judd [28] stated that "the processes by means of which an observer adapts to the illuminant or discounts most of the effect of non-daylight illumination are complicated; they are known to be partly retinal and partly cortical".

2.4.3 Von Kries Chromatic Adaptation

The von Kries coefficient law is the oldest and widely used to quantify chromatic adaptation. In 1902, von Kries [29] assumed that, although the responses of the three cone types (RGB)[2] are affected differently by chromatic adaptation, the spectral sensitivities of each of the three cone mechanisms remain unchanged. Hence, chromatic adaptation can be considered as a reduction of sensitivity by a constant factor for each of the three cone mechanisms. The magnitude of each factor depends upon the colour of the stimulus to which the observer is adapted. The relationship, given in (2.2), is known as the von Kries coefficient law.

$$R_c = \alpha \cdot R,$$
$$G_c = \beta \cdot G,$$
$$B_c = \gamma \cdot B, \tag{2.2}$$

where R_c, G_c, B_c and R, G, B are the cone responses of the same observer, but viewed under test and reference illuminants, respectively. α, β and γ are the von Kries coefficients corresponding to the reduction in sensitivity of the three cone mechanisms due to chromatic adaptation. These can be calculated using (2.3).

$$\alpha = \left(\frac{R_{wr}}{R_w}\right); \qquad \beta = \left(\frac{G_{wr}}{G_w}\right); \qquad \gamma = \left(\frac{B_{wr}}{B_w}\right), \tag{2.3}$$

where

$$\frac{R}{R_w} = \frac{R_c}{R_{wr}}, \qquad \frac{G}{G_w} = \frac{G_c}{G_{wr}}, \qquad \frac{B}{B_w} = \frac{B_c}{B_{wr}}, \tag{2.4}$$

---

[2]In this chapter the RGB symbols will be used for the cone fundamentals, in other chapters the reader will find the LMS symbols. The use of RGB here should not be confused with the *RGB* primaries used in visual colour matching.

Here R_{wr}, G_{wr}, B_{wr}, and R_{w}, G_{w}, B_{w} are the cone responses under the reference and test illuminants, respectively. Over the years, various CATs have been developed but most are based on the von Kries coefficient law.

2.4.4   Advanced Cats: Bradford, CMCCAT20000 and CAT02

In 1985, Lam and Rigg accumulated a set of corresponding colour pairs. They used 58 wool samples that had been assessed twice by a panel of five observers under D65 and A illuminants. The memory-matching technique was used to establish pairs of corresponding colours. In their experiment, a subgroup of colours was first arranged in terms of chroma and hue, and each was then described using Munsell H V/C coordinates. The data in H V/C terms, were then adjusted and converted to CIE 1931 XYZ values under illuminant C. Subsequently, the data under illuminant C were transformed to those under illuminant D65 using the von Kries transform. They used this set of data to derive a chromatic transform known as BFD transform now. The BFD transform can be formulated as the following:

2.4.4.1   Bfd Transform [20]

Step 1:

$$
\begin{pmatrix} R \\ G \\ B \end{pmatrix} = \frac{1}{Y} M_{\mathrm{BFD}} \begin{pmatrix} X \\ Y \\ Z \end{pmatrix} \text{ with } M_{\mathrm{BFD}} = \begin{pmatrix} 0.8951 & 0.2664 & 0.1614 \\ -0.7502 & 1.7135 & 0.0367 \\ 0.0389 & -0.0685 & 1.0296 \end{pmatrix}.
$$

Step 2:

$$
\begin{pmatrix} R_{\mathrm{c}} \\ G_{\mathrm{c}} \\ B_{\mathrm{c}} \end{pmatrix} = \begin{pmatrix} R_{\mathrm{wr}}/R_{\mathrm{w}} & & \\ & G_{\mathrm{wr}}/G_{\mathrm{w}} & \\ & & B_{\mathrm{wr}}/B_{\mathrm{w}}^{p} \end{pmatrix} \begin{pmatrix} R \\ G \\ \mathrm{sign}(B)|B|^{p} \end{pmatrix} \text{ with }
$$

$$
p = (B_{\mathrm{w}}/B_{\mathrm{wr}})^{0.0834}.
$$

Step 3:

$$
\begin{pmatrix} X_{\mathrm{c}} \\ Y_{\mathrm{c}} \\ Z_{\mathrm{c}} \end{pmatrix} = M_{\mathrm{BFD}}^{-1} \begin{pmatrix} Y R_{\mathrm{c}} \\ Y G_{\mathrm{c}} \\ Y B_{\mathrm{c}} \end{pmatrix}.
$$

Note that the BFD transform is a nonlinear transform. The exponent p in step 2 for calculating the blue corresponding spectral response can be considered as a modification of the von Kries type of transform. The BFD transform performs much better than the von Kries transform. In 1997, Luo

and Hunt [30] in 1997 modified the step 2 in the above BFD transform by introducing an adaptation factor D. The new step 2 becomes,

Step 2'

$$\begin{pmatrix} R_c \\ G_c \\ B_c \end{pmatrix} = \begin{pmatrix} [D(R_{wr}/R_w) + 1 - D]R \\ [D(G_{wr}/G_w) + 1 - D]G \\ [D(B_{wr}/B_w^p) + 1 - D]\text{sign}(B)|B|^p \end{pmatrix},$$

where

$$D = F - F/[1 + 2L_A^{1/4} + L_A^2/300].$$

The transform consisting of Step 1, Step 2' and Step 3 was then recommended by the colour measurement committee (CMC) of the society of dyers and colourists (SDC) and, hence, was named as the CMCCAT97. This transform is included in the CIECAM97s for describing colour appearance under different viewing conditions. The BFD transform was originally derived by fitting only one data set, Lam and Rigg. Although it gave a reasonably good fit to many other data sets, it predicted badly the McCann data set. In addition, the BFD and CMCCAT97 include an exponent *p* for calculating the blue corresponding spectral response. This causes uncertainty in reversibility and complexity in the reverse mode. Li et al. [31] addressed this problem and provided a solution by including an iterative approximation using the Newton method. However, this is unsatisfactory in imaging applications where the calculations need to be repeated for each pixel. Li et al. [27] gave a linearisation version by optimising the transform to fit all the available data sets, rather than just the Lam and Rigg set. The new transform, named CMCCAT2000, is given below.

2.4.4.2 Cmccat2000

Step 1:

$$\begin{pmatrix} R \\ G \\ B \end{pmatrix} = M_{00} \begin{pmatrix} X \\ Y \\ Z \end{pmatrix} \text{ with } M_{00} = \begin{pmatrix} 0.7982 & 0.3389 & -0.1371 \\ -0.5918 & 1.5512 & 0.0406 \\ 0.0008 & 0.0239 & 0.9753 \end{pmatrix}.$$

Step 2:

$$\begin{pmatrix} R_c \\ G_c \\ B_c \end{pmatrix} = \begin{pmatrix} [D(Y_w/Y_{wr})(R_{wr}/R_w) + 1 - D]R \\ [D(Y_w/Y_{wr})(G_{wr}/G_w) + 1 - D]G \\ [D(Y_w/Y_{wr})(B_{wr}/B_w) + 1 - D]B \end{pmatrix}$$

with

$$D = F\{0.08\log_{10}[0.5(L_{A1} + L_{A2})] + 0.76 - 0.45(L_{A1} - L_{A2})/(L_{A1} + L_{A2})\}.$$

Step 3:

$$\begin{pmatrix} X_c \\ Y_c \\ Z_c \end{pmatrix} = M_{00}^{-1} \begin{pmatrix} R_c \\ G_c \\ B_c \end{pmatrix}.$$

The CMCCAT2000 not only overcomes all the problems with respect to reversibility discussed above, but also gives a more accurate prediction than other transforms of almost all the available data sets.

During and after the development of the CMCCAT2000, scientists decided to drop the McCann et al. data set because the experiment was carried out under a very chromatic adapting illuminant. Its viewing condition is much different from all the other corresponding data sets. Hence, it would be better to optimising the linear chromatic adaptation transform via fitting all the corresponding data sets without the McCann et al. data set. The new matrix obtained by the authors, now named the CAT02 matrix, is given by

$$M_{02} = \begin{pmatrix} 0.7328 & 0.4296 & -0.1624 \\ -0.7036 & 1.6975 & 0.0061 \\ 0.0030 & 0.0136 & 0.9834 \end{pmatrix},$$

which was first included in the appendix of our paper [32] in 2002. At the same time, Nathan Moroney (Chair of CIETC8-01 at that time) proposed a new formula for D function:

$$D = F \left[1 - \frac{1}{3.6} e^{\frac{-L_A - 42}{92}} \right]. \tag{2.5}$$

The CMCCAT2000 with the new matrix and D formula given by (2.5) becomes the CAT02.

At a later stage, CIE TC 8-01 *Colour Appearance Modelling for Colour Management Systems* had to choose a linear chromatic transform for CIECAM02. Multiple candidates such as CMCCAT2000 [27], the sharp chromatic transform [33] developed by Finlayson et al., and CAT02 [6–8] were proposed for use as a von Kries type transform. All had similar levels of performance with respect to the accuracy of predicting various combinations of previously derived sets of corresponding colours. In addition to the sharpening of the spectral sensitivity functions, considerations used to select the CIE transform included the degree of backward compatibility with CIECAM97s and error propagation properties by combining the forward and inverse linear CAT, and the data sets which were used during the optimisation process. Finally, CAT02 was selected because it is compatible with CMCCAT97 and was optimised using all available data sets except the McCann et al. set, which includes a very chromatic adapting illuminant.

Figure 2.6 illustrates 52 pairs of corresponding colours predicted by CIECAM02 (or its chromatic adaptation transform, CAT02) from illuminant A (open circles of vectors) to S_E (open ends of vectors) plotted in the CIE $u'v'$ chromaticity diagram for the 2° observer. The open circle colours have a value of L^* equal
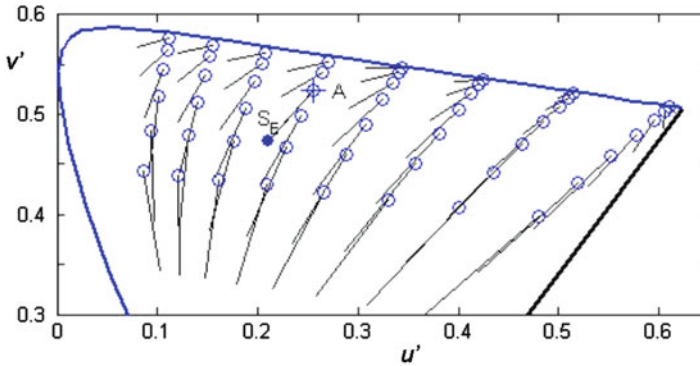
Fig. 2.6 The corresponding colours predicted by the CIECAM02 from illuminant A (*open circles* of vectors) to illuminant S_E (*open ends* of vectors) plotted in CIE $u'v'$ chromaticity diagram for the CIE 1931 standard colorimetric observer. The plus (+) and the dot (•) represent illuminants A and S_E, respectively

to 50 according to CIELAB under illuminant A. These were then transformed by the model to the corresponding colours under illuminant S_E (the equi-energy illuminant). Thus, the ends of each vector represent a pair of corresponding colours under the two illuminants. The input parameters are (the luminance of adapting field) $L_A = 63.7 \, \text{cd/m}^2$ and average surround. The parameters are defined in the Appendix.

The results show that there is a systematic pattern, i.e., for colours below v' equal to 0.48 under illuminant A the vectors are predicted towards the blue direction under the illuminant S_E. For colours outside the above region, the appearance change is in a counterclockwise direction, i.e., red colours shift to yellow, yellow to green and green to cyan as the illuminant changes from A to S_E.

2.5 Colour Appearance Phenomena

This section describes a number of colour appearance phenomena studied by various researchers in addition to the chromatic adaptation as described in the earlier section. The following effects are also well understood.

2.5.1 Hunt Effect

Hunt [34] studied the effect of light and dark adaptation on colour perception and collected data for corresponding colours via a visual colorimeter using the haploscopic matching technique, in which each eye was adapted to different viewing conditions and matches were made between stimuli presented in each eye.

The results revealed a visual phenomena known as Hunt effect [34]. It refers to the fact that the colourfulness of a colour stimulus increases due to the increase of luminance. This effect highlights the importance of considering the absolute luminance level in colour appearance models, which is not considered in traditional colorimetry.

2.5.2 Stevens Effect

Stevens and Stevens [35] asked observers to make magnitude estimations of the brightness of stimuli across various adaptation conditions. The results showed that the perceived brightness contrast increased with an increase in the adapting luminance level according to a power relationship.

2.5.2.1 Surround Effect

Bartleson and Breneman [36] found that the perceived contrast in colourfulness and brightness increased with increasing illuminance level from dark surround, dim surround to average surround. This is an important colour appearance phenomenon to be modelled, especially for the imaging and graphic arts industries where, on many occasions, it is required to reproduce images on different media under quite distinct viewing conditions.

2.5.3 Lightness Contrast Effect

The lightness contrast effect [37] reflects that the perceived lightness increases when colours are viewed against a darker background and vice versa. It is a type of simultaneous contrast effect considering the change of colour appearance due to different coloured backgrounds. This effect has been widely studied and it is well known that a change in the background colour has a large impact on the perception of lightness and hue. There is some effect on colourfulness, but this is much smaller than the effect on lightness and hue [37].

2.5.4 Helmholtz–Kohlrausch Effect

The Helmholtz–Kohlrausch [38] effect refers to a change in the brightness of colour produced by increasing the purity of a colour stimulus while keeping its luminance constant within the range of photopic vision. This effect is quite small compared with others and is not modelled by CIECAM02.

2.5.5 Helson–Judd Effect

When a grey scale is illuminated by a light source, the lighter neutral stimuli will exhibit a certain amount of the hue of the light source and the darker stimuli will show its complementary hue, which is known as the Helson–Judd effect [39]. Thus for tungsten light, which is much yellower than daylight, the lighter stimuli will appear yellowish, and the darker stimuli bluish. This effect is not modelled by CIECAM02.

2.6 Recent Developments of CIECAM02

Recently, several extensions to the CIECAM02 have been made, which have widened the applications of the CIECAM02. In this section, the extensions for predicting colour discrimination data sets, size effects and unrelated colour appearance in the mesopic region. Besides, recent developments from CIETC8-11 will be reported as well.

2.6.1 CIECAM02-Based Colour Spaces

CIECAM02 [6, 7] includes three attributes in relation to the chromatic content: chroma (C), colourfulness (M) and saturation (s). These attributes together with lightness (J) and hue angle (h) can form three colour spaces: J, a_C, b_C, J, a_M, b_M and J, a_s, b_s where

$$a_C = C \cdot \cos(h) \qquad a_M = M \cdot \cos(h) \qquad a_s = s \cdot \cos(h)$$
$$b_C = C \cdot \sin(h) \,, \qquad b_M = M \cdot \sin(h) \,, \qquad b_s = s \cdot \sin(h).$$

It was also found [40] that the CIECAM02 space is more uniform than the CIELAB space. Thus, the CIECAM02 space is used as a connection space for the gamut mapping in the colour management linked with the ICC profile [41, 42]. Further attempts have been also made by the authors to extend CIECAM02 for predicting available colour discrimination data sets, which include two types, for Large and Small magnitude Colour Differences, designated by LCD and SCD, respectively. The former includes six data sets with a total 2,954 pairs, having an average 10 ΔE_{ab}^* units over all the sets. The SCD data with a total of 3,657 pairs having an average 2.5 ΔE_{ab}^* units, are a combined data set used to develop the CIE 2000 colour difference formula: CIEDE2000[3].

Li et al. [43] found that a colour space derived using J, a_M, b_M gave the most uniform result when analysed using the large and small colour difference data sets. Hence, various attempts [9, 43] were made to modify this version of CIECAM02 to fit all available data sets. Finally, a simple, generic form, (2.6) was found that

Table 2.2 The coefficients for CAM02-LCD, CAM02-SCD and CAM02-UCS

Versions	CAM02 -LCD	CAM02-SCD	CAM02-UCS
K_L	0.77	1.24	1.00
c_1	0.007	0.007	0.007
c_2	0.0053	0.0363	0.0228

adequately fitted all available data.

$$J' = \frac{(1 + 100 \cdot c_1) \cdot J}{1 + c_1 \cdot J},$$

$$M' = (1/c_2) \cdot \ln(1 + c_2 \cdot M), \tag{2.6}$$

where c_1 and c_2 are constants given in Table 2.2.

The corresponding colour space is J', a'_M, b'_M where $a'_M = M' \cdot \cos(h)$, and $b'_M = M' \cdot \sin(h)$. The colour difference between two samples can be calculated in J', a'_M, b'_M space using (2.7).

$$\Delta E' = \sqrt{(\Delta J'/K_L)^2 + \Delta a'^2_M + \Delta b'^2_M}, \tag{2.7}$$

where $\Delta J', \Delta a'_M$ and $\Delta b'_M$ are the differences of J', a'_M and b'_M between the "standard" and "sample" in a pair. Here, K_L is a lightness parameter and is given in Table 2.2.

Three colour spaces named CAM02-LCD, CAM02-SCD and CAM02-UCS were developed for large, small and combined large and small differences, respectively. The corresponding parameters in (2.6) and (2.7) are listed in Table 2.2.

The three new CIECAM02 based colour spaces, together with the other spaces and formulae were also tested by Luo et al. [9]. The results confirmed that CAM02-SCD and CAM02-LCD performed the best for small and large colour difference data sets. When selecting one UCS to evaluate colour differences across a wide range, CAM02-UCS performed the second best across all data sets. The authors have been recommending using CAM02-UCS for all applications.

Figure 2.7 shows the relationship between *CIECAM02 J* and *CAM02-UCS J'* and Fig. 2.8 shows the relationship between *CIECAM02 M* and *CAM02-UCS M'*. It can be seen that CIECAM02 J is less than CAM02-UCS J' except at the two ends, while CIECAM02 M is greater than CAM02-UCS M' except when $M = 0$. Thus in order to have a more uniform space, CIECAM02 J should be increased and CIECAM02 M should be decreased.

The experimental colour discrimination ellipses used in the previous studies [44, 45] were also used for comparing different colour spaces. Figures 2.9 and 2.10 show the ellipses plotted in CIELAB and CAM02-UCS spaces, respectively. The size of the ellipse was adjusted by a single factor in each space to ease visual comparison. For perfect agreement between the experimental results and a uniform colour space, all ellipses should be constant radius circles. Overall, it can be seen that the ellipses in CIELAB (Fig. 2.9) are smaller in the neutral region and gradually increase in size as chroma increases. In addition, the ellipses are

Fig. 2.7 The *full line* shows
the relationship between *J*
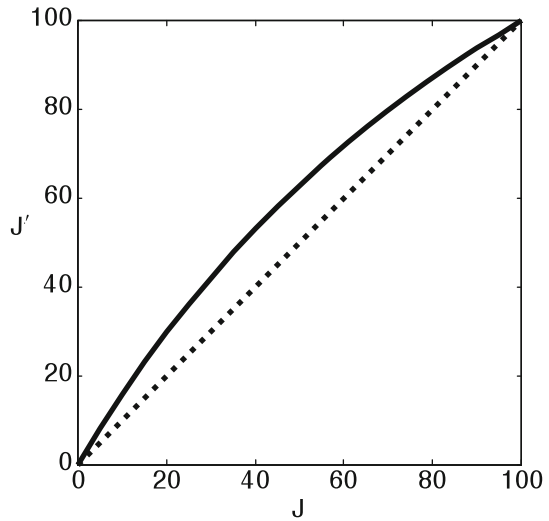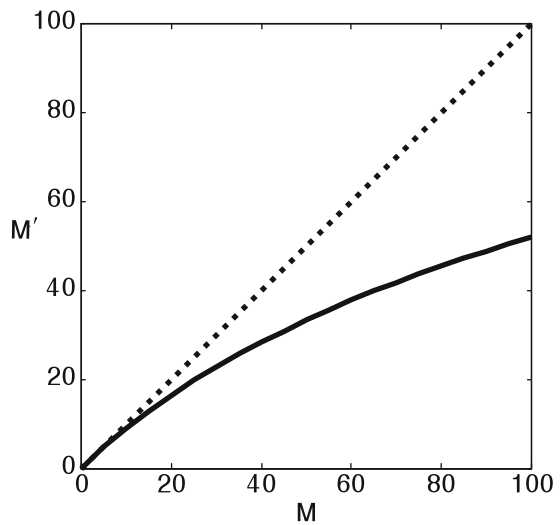and *J′* and the *dotted line* is
the 45° line

Fig. 2.8 The *full line* shows
the relationship between M
and M′ and the *dotted line* is
the 45° line

orientated approximately towards the origin except for those in the blue region in
CIELAB space. All ellipses in CAM02-UCS (Fig. 2.10) are approximately equal-
sized circles. In other words, the newly developed CAM02-UCS is much more
uniform than CIELAB.

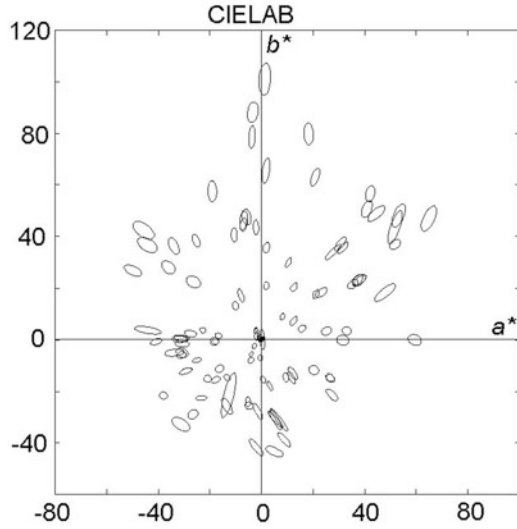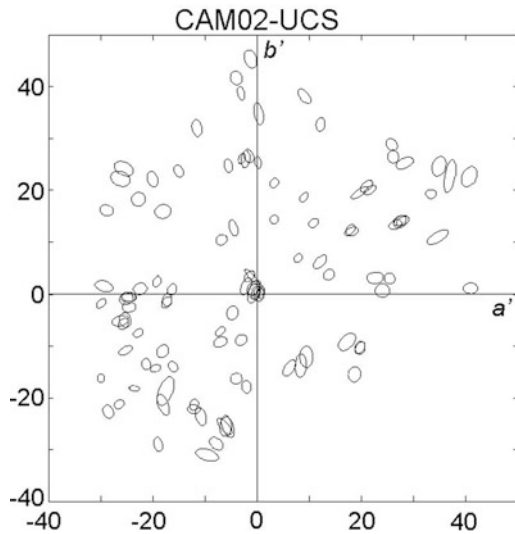**Fig. 2.9** Experimental chromatic discrimination ellipses plotted in CIELAB

Fig. 2.10 Experimental chromatic discrimination ellipses plotted in CAM02-UCS

2.6.2   Size Effect Predictions Based on CIECAM02

The colour size effect is a colour appearance phenomenon [10–12], in which the colour appearance changes according to different sizes of the same colour stimulus. The CIE 1931 (2°) and CIE 1964 (10°) standard colorimetric observers were recommended by the CIE to represent human vision in smaller and larger than 4° viewing fields, respectively [2]. However, for a colour with a large size, such as over 20° viewing field, no standard observer can be used. The current
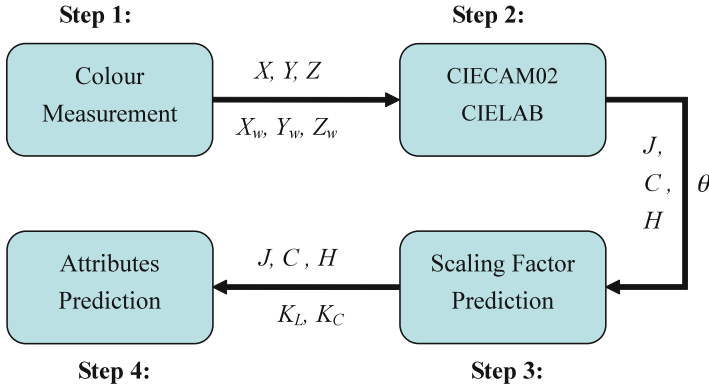
Fig. 2.11 The flow chart of size effect correction model based on CIECAM02

CIECAM02 is capable of predicting human perceptual attributes under various viewing conditions. However, it cannot predict the colour size effect. The size effect has been interested in many applications. For example, in the paint industry, the paints purchased in stores usually do not appear the same comparing between those shown in the packaging and painted onto the walls in a real room. This also causes great difficulties for homeowners, interior designers and architects when they select colour ranges. Furthermore, the display size tends to become larger. Colour size effect has also been greatly interested by display manufacturers in order to precisely reproduce or to enhance the source images on different sizes of colour displays.

With the above problems in mind, the CIE established a technical committee, TC1-75, *A comprehensive model for colour appearance* with one of aims to take colour size effect into account in the CIECAM02 colour appearance model [7]. In the recent work of Xiao et al. [10–12], six different sizes from 2° to 50° of same colours were assessed by a panel of observers using colour-matching method to match surface colours using a CRT display. The colour appearance data were accumulated in terms of CIE tristimulus values. A consistent pattern of colour appearance shifts was found according to different sizes for each stimulus. The experimental results showed that attributes of lightness and chroma increase with the increase of the physical size of colour stimulus. But the hue (composition) is not affected by the change of physical size of colour stimulus. Hence, a model based on CIECAM02 for predicting the size effect was derived. The model has the general structure shown in Fig. 2.11.

Step 1 calculates or measures tristimulus values X, Y, Z of a 2° stimulus size under a test illuminant X_W, Y_W, Z_W, and provides a target stimulus size θ; next, Step 2 predicts the appearance attributes J, C and H using CIECAM02 for colours with 2° stimulus size; and Step 3 computes the scaling factors K_J and K_C via the following formulae:

$$K_J = -0.007\theta + 1.1014,$$

$$K_C = 0.008\theta + 0.94.$$

Fig. 2.12 The size effect corrected attributes J'' vs CIECAM02 J under viewing angles being 25°, (*thick solid line*), 35° (*dotted line*) and 45° (*dashed line*), respectively. The *thin solid line* is the 45° line where $J = J''$
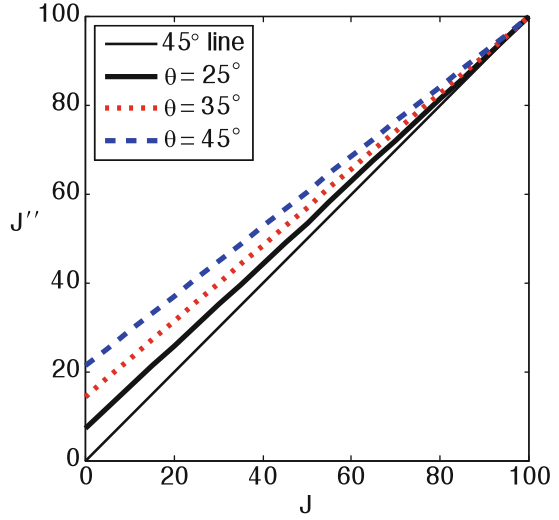
Finally in Step 4, the colour appearance attributes J'', C'' and H'' for the target stimulus size θ are predicted using the formulae:

$$J'' = 100 + K_{\mathrm{J}} \times (J - 100), \tag{2.8}$$

$$C'' = K_{\mathrm{C}} \times C, \tag{2.9}$$

$$H'' = H. \tag{2.10}$$

The earlier experimental results [10] were used to derive the above model.

Figure 2.12 shows the corrected attributes J'' of 25°, 35° and 45°, respectively, plotted against J at 2° viewing field. The thick solid line is the corrected J'' when viewing field is 25°; the dotted line corresponds to the J'' with viewing angle being 35°. The dashed line is the J'' with viewing angle of 45°. The thin solid line is the 45° line where $J = J''$. The trend is quite clear as shown in Fig. 2.12, i.e., an increase of lightness for a larger viewing field. For example, when $J = 60$ with a size of 2°, J'' values are 62.9, 65.7 and 68.5 for sizes of 25°, 35° and 45°, respectively. However, when $J = 10$ with a size of 2°, J''s become 16.6, 22.9 and 29.2 for 25°, 35° and 45°, respectively. This implies that the large effect is mainly occurred for the dark colour region.

Figure 2.13 shows the corrected attributes C'' of 25°, 35° and 45°, respectively plotted against C at 2° viewing field. Vertical axis is the size effect corrected C''. The thick solid line is the corrected C'' when viewing angle is 25°; the dotted line corresponds to the C'' with viewing angle being 35°. The dashed line is the C'' with viewing angle of 45°. The thin solid line is the 45° line where $C = C''$. Again, a clear trend in Fig. 2.13 is shown that an increase of chroma for a larger viewing field. For example, when C is 60 with a size of 2°, C'' values are 68.4, 73.2 and 78.0 for sizes

Fig. 2.13 The size effect corrected attributes C'' vs CIECAM02 C under viewing being 25°, (*thick solid line*), 35° (*dotted line*) and 45° (*dashed line*), respectively. The *thin solid line* is the 45° line where $C = C''$
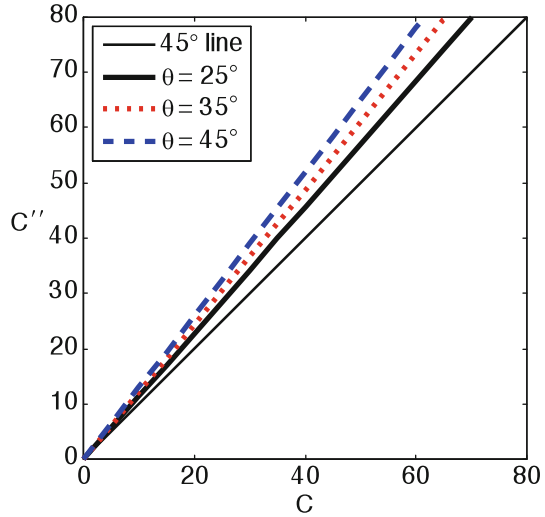
of 25°, 35° and 45°, respectively. However, when C is 10 with a size of 2°, C''s become 11.4, 12.2 and 13.0 for 25°, 35° and 45°, respectively. This implies that the large effect in mainly occurrs in the high chroma region.

2.6.3 Unrelated Colour Appearance Prediction Based on CIECAM02

As mentioned at the beginning of this chapter, unrelated colours are important in relation to safety issues (such as night driving). It includes signal lights, traffic lights and street lights, viewed on a dark night. These colours are important in connection with safety issues. The CIECAM02 was derived for predicting colour appearance for related colours and it cannot be used for predicting unrelated colour appearance. The CAM97u derived by Hunt [46] can be used for predicting unrelated colour appearance. However, the model was not tested since there was no available visual data for unrelated colours. Fu et al. [13] carried out the research work recently. They accumulated a set of visual data using the configuration in Fig. 2.4. The data were accumulated for the colour appearance of unrelated colours under photopic and mesopic conditions. The effects of changes in luminance level and stimulus size on appearance were investigated. The method used was magnitude estimation of brightness, colourfulness and hue. Four luminance levels (60, 5, 1 and 0.1, cd/m^2) were used. For each of the first three luminance levels, two stimulus sizes (10°, 2°, 1° and 0.5°) were used. Ten observers judged 50 unrelated colours. A total of 17,820 estimations were made. The observations were carried out in a completely darkened room, after about 20 min adaptation; each test colour was presented on

its own. Brightness and colourfulness were found to decrease with decreases of both luminance level and stimulus size. The results were used to further extend CIECAM02 for predicting unrelated colours under both photopic and mesopic conditions. The model includes parameters to reflect the effects of luminance level and stimulus size. The model is described below:

Inputs:

Measure or calculate the luminance L and chromaticity x,y of the test colour stimulus corresponding to CIE colour-matching functions (2° or 10°). The parameters are the same as CIECAM02 except that the test illuminant is equal energy illuminant (S_E, i.e., $X_W = Y_W = Z_W = 100$), and $L_A = 1/5$ of the adapting luminance, and the surround parameters are set as those under the dark viewing condition. As reported by Fu et al. [13], when there is no reference illuminant to compare with (such as assessing unrelated colours), S_E illuminant can be used by assuming no adaptation takes place for unrelated viewing condition.

Step 1: Using the CIECAM02 (Steps 0–8, Step 10, ignore the calculation of Q and s) to predict the (cone) achromatic signal A, colourfulness (M) and hue (H_C).

Step 2: Modify the achromatic signal A since there is a contribution from rod response using the formula:

$$A_{\text{new}} = A + k_A A_S \text{ with } A_S = (2.26L)^{0.42}.$$

Here, k_A depends on luminance level and viewing angle size of the colour stimulus.

Step 3: Modify the colourfulness M predicted from CIECAM02 using the following formula:

$$M_{\text{new}} = k_M M.$$

Here, k_M depends on luminance level and viewing angle size of the colour stimulus.

Step 4: Predict the new brightness using the formula:

$$Q_{\text{new}} = A_{\text{new}} + M_{\text{new}}/100.$$

Outputs: Brightness Q_{new}, colourfulness M_{new} and hue composition H_C.

Note that the hue composition H_C is the same as predicted by CIECAM02. The above model was tested using the visual data [13].

Figure 2.14 shows the brightness and colourfulness changes for a red colour of medium saturation (relative to S_E, $h_{\text{uv}} = 355°$, and $s_{\text{uv}} = 1.252$) as predicted by the new model under different luminance levels. The luminance levels were varied from

Fig. 2.14 The brightness and colourfulness predicted by the new model for a sample varying in luminance level with 2° stimulus size
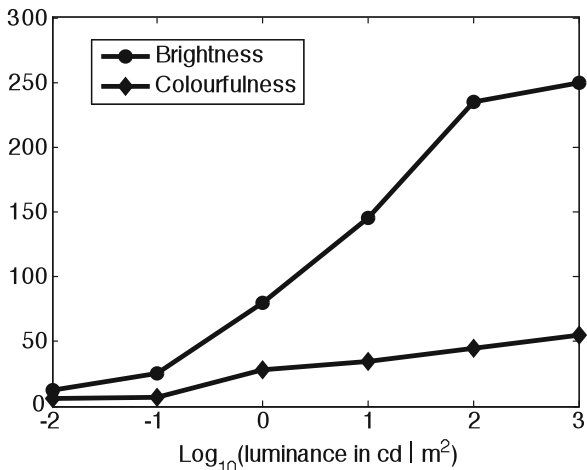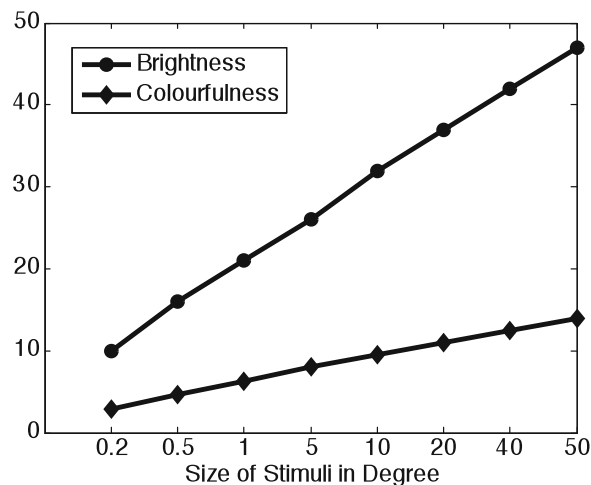

Fig. 2.15 The brightness and colourfulness predicted by the new model for a sample varying in stimulus size at 0.1 cd/m² luminance level

0.01 to 1000 cd/m², and L_A was set at one fifth of these values. The ratio Y_b/Y_w set at 0.2. Figure 2.15 shows the brightness and colourfulness changes, for the same red colour, predicted by the new model for different stimulus sizes ranging from 0.2° to 40°. The luminance level (L) was set at 0.1 cd/m². It can be seen that brightness and colourfulness increase when luminance increases up to around 100 cd/m², and they also increase when stimulus size increases. These trends reflect the phenomena found in Fu et al.'s study, i.e. when luminance level increases, colours become brighter and more colourful, and larger colours appear brighter and more colourful than smaller sized colours; however, below a luminance of 0.1 cd/m² and above a luminance of 60 cd/m², and below a stimulus size of 0.5° and above a stimulus size of 10^0, these results are extrapolations, and must be treated with caution.

2.6.4 Problems with CIECAM02

Since the recommendation of the CIECAM02 colour appearance model [6, 7] by CIE TC8-01 Colour appearance modelling for colour management systems, it has been used to predict colour appearance under a wide range of viewing conditions, to specify colour appearance in terms of perceptual attributes, to quantify colour differences, to provide a uniform colour space and to provide a profile connection space for colour management. However, some problems have been identified and various approaches have been proposed to repair the model to enable it to be used in practical applications. During the 26th session of the CIE, held in Beijing in July 2007, a Technical Committee, TC8-11 CIECAM02 Mathematics, was formed to modify or extend the CIECAM02 model in order to satisfy the requirements of a wide range of industrial applications. The main problems that have been identified can be summarised as follows:

1. Mathematical failure for certain colours
2. The CIECAM02 colour domain is smaller than that of ICC profile connection space
3. The HPE matrix
4. The brightness function

Each problem will be reviewed in turn and then a possible solution that either repairs the problem or extends the model will be given as well. Note that all notations used in this paper have the same meaning as those in CIE Publication 159 [7].

2.6.4.1   Mathematical Failure

It has been found that the Lightness function:

$$J = 100(A/A_{\mathrm{w}})^{cz}$$

gives a problem for some colours. In fact Li and Luo [47] have shown that $A_{\mathrm{w}} > 0$, but for some colours, the achromatic signal

$$A = \left[2R'_a + G'_a + (1/20)B'_a - 0.305\right] \mathrm{N_{bb}}$$

can be negative; thus, the ratio in the bracket for the J function is negative which gives problem when computing J. At the beginning, it has been suggested that the source of the problem is the CAT02 transform which, for certain colours, predicts negative tristimulus values. Several approaches have been made on modifying the CAT02 matrix. Brill and Süsstrunk [48–50] found that the red and green CAT02 primaries lie outside the HPE triangle and called this as the "Yellow-Blue" problem. They suggested that the last row of the CAT02 matrix can be changed to 0, 0, 1. The changed matrix is denoted by M_{BS}. It has been found that for certain colours, using

matrix M_{BS} works well, but using matrix M_{02} does not. However, this repair seems to correct neither the prediction of negative tristimulus values for the CAT02 nor the failure of CIECAM02.

Another suggestion is equivalent to set $R'_a \geq 0.1$, i.e., if $R'_a < 0.1$, then set $R'_a = 0.1$, if $R'_a \geq 0.1$, then R'_a does not change. Similar considerations are applied to G'_a and B'_a. Thus, under this modification, the achromatic signal A is non-negative. However, this change causes new problem with the inverse model.

Li et al. [51] gave a mathematical approach for obtaining CAT02 matrix. The approach has two constraints. The first one is to ensure the CAT02 predict corresponding colours with non-negative tristimulus values under all the illuminants considered for all colours located on or inside the CIE chromaticity locus. The second one is to fit all the corresponding colour data sets. This approach indeed ensures the CAT02 with the new matrix predicts corresponding colours with non-negative tristimulus values which is important in many applications. However, this approach does not solve the mathematical failure problem for the CIECAM02.

Recently, Li et al. [14] proposed a mathematical approach for ensuring the achromatic signal A being non-negative, at the same time the CIECAM02 should fit all the colour appearance data sets. Finally the problem is formulated as a constrained non-linear optimisation problem. By solving the optimization problem, a new CAT02 matrix was derived. With this new matrix, it was found that the mathematical failure problem of the CIECAM02 is overcome for all the illuminants considered. Besides, they also found that if the CAT02 with the HPE matrix, the mathematical failure problem is also overcome for any illuminant. More important, the HPE matrix makes the CIECAM02 simpler. All the new matrices are under the evaluation of the CIE TC8-11.

2.6.4.2 CIECAM02 Domain is Smaller than that of ICC Profile Connection Space

The ICC has developed and refined a comprehensive and rigorous system for colour management [52]. In an ICC colour management work flow, an input colour is mapped from a device colour space into a colorimetric description for specific viewing conditions (called the profile connection space—PCS). The PCS is selected as either CIE XYZ or Lab space under illuminant D50 and the 2° observer. Generally speaking, the input and output devices have different gamuts and, hence, a gamut mapping is involved. Gamut mapping in XYZ space can cause problems because of the perceptual non-uniformity of that colour space. Lab space is not a good space for gamut mapping since lines of constant hue are not generally straight lines, especially in the blue region [53]. CIECAM02 has been shown to have a superior perceptual uniformity as well as better hue constancy [40]. Thus, the CIECAM02 space has been selected as the gamut mapping space.

However, the ICC PCS can contain non-physical colours, which cause problems when transforming to CIECAM02 space, for example, in the Lightness function J defined above and the calculation of the parameter defined by

$$t = \frac{(50000/13)N_c N_{cb} e_t (a^2 + b^2)^{1/2}}{R'_a + G'_a + (21/20)B'_a}.$$

When computing J, the value of A can be negative and when computing t, $R'_a + G'_a + (21/20)B'_a$ can be or near zero. One approach [41, 42] to solving these problems is to find the domain of CIECAM02 and to pre-clip or map colour values outside of this domain to fall inside or on this domain boundary, and then the CIECAM02 model can be applied without any problems. The drawbacks of this approach are that a two step transformation is not easily reversible to form a round trip solution and clipping in some other colour space would seem to defeat much of the purpose of choosing CIECAM02 as the gamut mapping space. Another approach [54] is to extend CIECAM02 so that it will not affect colours within its normal domain but it will still work, in the sense of being mathematically well defined, for colours outside its normal domain. To investigate this, the J function and the non-linear post-adaptation functions in the CIECAM02 were extended. Furthermore, scaling factors were introduced to avoid the difficulty in calculating the t value. Simulation results showed this extension of CIECAM02 works very well and full details can be found in the reference [54]. This approach is also under the evaluation of the CIE TC8-11.

2.6.4.3 The HPE Matrix;

Kuo et al. [55] found that the sum of the first row of the HPE matrix (eq. (12)) is different from unity, which causes a non-zero value of a and b when transforming the test light source to the reference (equal-energy) light source under full adaptation. Hence, a slight change to the matrix should be made. For example, the top right element -0.07868 could be changed to -0.07869. In fact, Kuo et al. [55] suggested changing each element in the first row slightly.

2.6.4.4 The Brightness Function

The brightness function of CIECAM02 is different from the brightness function of the older CIECAM97s model. The major reason for the change [56] was because of the correction to the saturation function (s). However, it has been reported that the brightness prediction of CIECAM02 does not correlate well with the appropriate visual data [57]. More visual brightness data is needed to clarify the brightness function.

2.7 Conclusion

This chapter describes the CIECAM02 in great details. Furthermore, more recent works have been introduced to extend its functions. Efforts were made to reduce the problems such as mathematical failure for the computation of the lightness attribute.

Overall, the CIECAM02 is capable of accurately predicting colour appearance under a wide range of viewing conditions. It has been proved to achieve successfully cross-media colour reproduction (e.g., the reproduction of an image on a display, on a projection screen or as hard copy) and is adopted by the Microsoft Company in their latest colour management system, window color system (WCS). With the addition of CAM02-UCS uniform colour space, size effect and unrelated colours, it will become a comprehensive colour appearance models to serve most of the applications.

Appendix: CIE Colour Appearance Model: CIECAM02

Part 1: The Forward Mode

Input: X, Y, Z (under test illuminant X_w, Y_w, Z_w)
Output: Correlates of lightness J, chroma C, hue composition H, hue angle h, colourfulness M, saturation s and brightness Q

    Illuminants, viewing surrounds set up and background parameters
    (See the note at the end of this Appendix for determining all parameters)

Adopted white in test illuminant: X_w, Y_w, Z_w
Background in test conditions: Y_b
(Reference white in reference illuminant: $X_{wr} = Y_{wr} = Z_{wr} = 100$, which are fixed in the model)
Luminance of test-adapting field (cd/m^2) : L_A
All surround parameters are given in Table 2.3 below
Note that for determining the surround conditions, see the note at the end of this Appendix. N_c and F are modelled as a function of c, and can be linearly interpolated as shown in the Fig. 2.16 below, using the above points

Step 0: Calculate all values/parameters which are independent of input samples

$$\begin{pmatrix} R_w \\ G_w \\ B_w \end{pmatrix} = M_{CAT02} \cdot \begin{pmatrix} X_w \\ Y_w \\ Z_w \end{pmatrix}, \quad D = F \cdot \left[1 - \left(\frac{1}{3.6} \right) \cdot e^{\left(\frac{-L_A - 42}{92} \right)} \right].$$
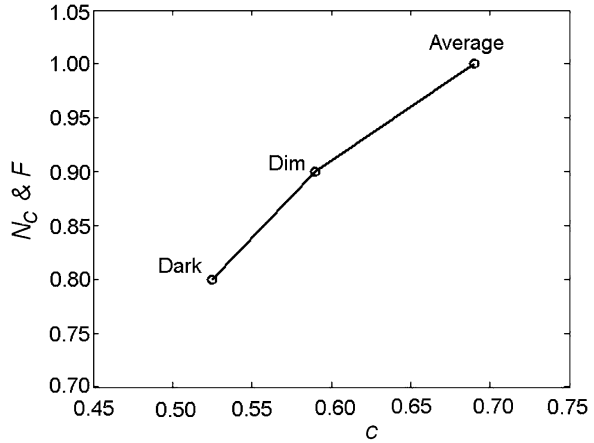
    Note if D is greater than one or less than zero, set it to one or zero, respectively.

$$D_R = D \cdot \frac{Y_w}{R_w} + 1 - D, \quad D_G = D \cdot \frac{Y_w}{G_w} + 1 - D, \quad D_B = D \cdot \frac{Y_w}{B_w} + 1 - D,$$

$$F_L = 0.2 \, k^4 \cdot (5L_A) + 0.1(1 - k^4)^2 \cdot (5L_A)^{1/3},$$

Table 2.3 Surround parameters

	F	c	N_c
Average	1.0	0.69	1.0
Dim	0.9	0.59	0.9
Dark	0.8	0.535	0.8

Fig. 2.16 N_c and F varies with c

where $k = \frac{1}{5 \cdot L_A + 1}$.

$$n = \frac{Y_b}{Y_w}, \quad z = 1.48 + \sqrt{n}, \quad N_{bb} = 0.725 \cdot \left(\frac{1}{n}\right)^{0.2}, \quad N_{cb} = N_{bb},$$

$$\begin{pmatrix} R_{wc} \\ G_{wc} \\ B_{wc} \end{pmatrix} = \begin{pmatrix} D_R \cdot R_w \\ D_G \cdot G_w \\ D_B \cdot B_w \end{pmatrix}, \quad \begin{pmatrix} R'_w \\ G'_w \\ B'_w \end{pmatrix} = M_{HPE} \cdot M_{CAT02}^{-1} \cdot \begin{pmatrix} R_{wc} \\ G_{wc} \\ B_{wc} \end{pmatrix},$$

$$M_{CAT02} = \begin{pmatrix} 0.7328 & 0.4296 & -0.1624 \\ -0.7036 & 1.6975 & 0.0061 \\ 0.0030 & 0.0136 & 0.9834 \end{pmatrix},$$

$$M_{HPE} = \begin{pmatrix} 0.38971 & 0.68898 & -0.07868 \\ -0.22981 & 1.18340 & 0.04641 \\ 0.00000 & 0.00000 & 1.00000 \end{pmatrix},$$

$$R'_{aw} = 400 \cdot \left(\frac{\left(\frac{F_L \cdot R'_w}{100}\right)^{0.42}}{\left(\frac{F_L \cdot R'_w}{100}\right)^{0.42} + 27.13} \right) + 0.1,$$

$$G'_{aw} = 400 \cdot \left(\frac{\left(\frac{F_L \cdot G'_w}{100} \right)^{0.42}}{\left(\frac{F_L \cdot G'_w}{100} \right)^{0.42} + 27.13} \right) + 0.1,$$

$$B'_{aw} = 400 \cdot \left(\frac{\left(\frac{F_L \cdot B'_w}{100} \right)^{0.42}}{\left(\frac{F_L \cdot B'_w}{100} \right)^{0.42} + 27.13} \right) + 0.1,$$

$$A_w = \left[2 \cdot R'_{aw} + G'_{aw} + \frac{B'_{aw}}{20} - 0.305 \right] \cdot N_{bb}.$$

Note that all parameters computed in this step are needed for the following calculations. However, they depend only on surround and viewing conditions; hence, when processing pixels of image, they are computed once for all. The following computing steps are sample dependent.

Step 1: Calculate (sharpened) cone responses (transfer colour-matching functions to sharper sensors)

$$\begin{pmatrix} R \\ G \\ B \end{pmatrix} = M_{CAT02} \cdot \begin{pmatrix} X \\ Y \\ Z \end{pmatrix},$$

Step 2: Calculate the corresponding (sharpened) cone response (considering various luminance level and surround conditions included in D; hence, in D_R, D_G and D_B)

$$\begin{pmatrix} R_c \\ G_c \\ B_c \end{pmatrix} = \begin{pmatrix} D_R \cdot R \\ D_G \cdot G \\ D_B \cdot B \end{pmatrix},$$

Step 3: Calculate the Hunt-Pointer-Estevez response

$$\begin{pmatrix} R' \\ G' \\ B' \end{pmatrix} = M_{HPE} \cdot M_{CAT02}^{-1} \cdot \begin{pmatrix} R_c \\ G_c \\ B_c \end{pmatrix},$$

Step 4: Calculate the post-adaptation cone response (resulting in dynamic range compression)

$$R'_a = 400 \cdot \left(\frac{\left(\frac{F_L \cdot R'}{100} \right)^{0.42}}{\left(\frac{F_L \cdot R'}{100} \right)^{0.42} + 27.13} \right) + 0.1.$$

If R' is negative, then

Table 2.4 Unique hue data for calculation of hue quadrature

	Red	Yellow	Green	Blue	Red
i	1	2	3	4	5
h_i	20.14	90.00	164.25	237.53	380.14
e_i	0.8	0.7	1.0	1.2	0.8
H_i	0.0	100.0	200.0	300.0	400.0

$$R'_a = -400 \cdot \left(\frac{\left(\frac{-F_L \cdot R'}{100} \right)^{0.42}}{\left(\frac{-F_L \cdot R'}{100} \right)^{0.42} + 27.13} \right)^{0.42} + 0.1$$

and similarly for the computations of G'_a, and B'_a, respectively.

Step 5: Calculate Redness–Greenness (a), Yellowness–Blueness (b) components and hue angle (h):

$$a = R'_a - \frac{12 \cdot G'_a}{11} + \frac{B'_a}{11},$$

$$b = \frac{(R'_a + G'_a - 2 \cdot B'_a)}{9},$$

$$h = \tan^{-1} \left(\frac{b}{a} \right)$$

make sure h between 0 and 360°.

Step 6: Calculate eccentricity (e_t) and hue composition (H), using the unique hue data given in Table 2.4; set $h' = h + 360$ if $h < h_1$, otherwise $h' = h$. Choose a proper $i (i = 1,2,3$ or $4)$ so that $h_i \leq h' < h_{i+1}$. Calculate

$$e_t = \frac{1}{4} \cdot \left[\cos \left(\frac{h' \cdot \pi}{180} + 2 \right) + 3.8 \right],$$

which is close to, but not exactly the same as, the eccentricity factor given in Table 2.4.

$$H = H_i + \frac{100 \cdot \frac{h' - h_i}{e_i}}{\frac{h' - h_i}{e_i} + \frac{h_{i+1} - h'}{e_{i+1}}}.$$

Step 7: Calculate achromatic response A

$$A = \left[2 \cdot R'_a + G'_a + \frac{B'_a}{20} - 0.305 \right] \cdot N_{bb}.$$

Step 8: Calculate the correlate of lightness

$$J = 100 \cdot \left(\frac{A}{A_w} \right)^{c \cdot z}.$$

Step 9: Calculate the correlate of brightness

$$Q = \left(\frac{4}{c}\right) \cdot \left(\frac{J}{100}\right)^{0.5} \cdot (A_w + 4) \cdot F_L^{0.25}.$$

Step 10: Calculate the correlates of chroma (C), colourfulness (M) and saturation (s)

$$t = \frac{\left(\frac{50000}{13} \cdot N_c \cdot N_{cb}\right) \cdot e_t \cdot \left(a^2 + b^2\right)^{1/2}}{R_a' + G_a' + \left(\frac{21}{20}\right) \cdot B_a'},$$

$$C = t^{0.9} \cdot \left(\frac{J}{100}\right)^{0.5} \cdot (1.64 - 0.29^n)^{0.73},$$

$$M = C \cdot F_L^{0.25},$$

$$s = 100 \cdot \left(\frac{M}{Q}\right)^{0.5}.$$

Part 2: The Reverse Mode

Input: J or Q; C, M or s; H or h
Output: X, Y, Z (under test illuminant X_w, Y_w, Z_w)

Illuminants, viewing surrounds and background parameters are the same as those given in the forward mode. See notes at the end of this Appendix calculating/defining the luminance of the adapting field and surround conditions.

Step 0: Calculate viewing parameters
Compute all $F_L, n, z, N_{bb} = N_{bc} = R_w, G_w, B_w, D, D_R, D_G, D_B, R_{wc}, G_{wc}, B_{wc}, R_w', G_w', B_w'$ $R_{aw}', G_{aw}', B_{aw}'$ and A_w using the same formulae as in Step 0 of the Forward model. They are needed in the following steps. Note that all data computed in this step can be used for all samples (e.g., all pixels for an image) under the viewing conditions. Hence, they are computed once for all. The following computing steps are sample dependent.

Step 1: Obtain J, C and h from H, Q, M, s
The entering data can be in different combination of perceived correlates, i.e., J or Q; C, M, or s; and H or h. Hence, the followings are needed to convert the others to J, C, and h.

Step 1–1: Compute J from Q (if start from Q)

$$J = 6.25 \cdot \left[\frac{c \cdot Q}{(A_w + 4) \cdot F_L^{0.25}}\right]^2.$$

Step 1–2: Calculate C from M or s

$$C = \frac{M}{F_L^{0.25}} \quad \text{(if start from } M\text{)}$$

$$Q = \left(\frac{4}{c}\right) \cdot \left(\frac{J}{100}\right)^{0.5} \cdot (A_w + 4.0) \cdot F_L^{0.25}$$

and $C = \left(\frac{s}{100}\right)^2 \cdot \left(\frac{Q}{F_L^{0.25}}\right)$ (if start from s)

Step 1–3: Calculate h from H (if start from H)

The correlate of hue (h) can be computed by using data in Table 2.4 in the Forward mode.

Choose a proper i $(i = 1,2,3 \text{ or } 4)$ so that $H_i \leq H < H_{i+1}$.

$$h' = \frac{(H - H_i) \cdot (e_{i+1}h_i - e_i \cdot h_{i+1}) - 100 \cdot h_i \cdot e_{i+1}}{(H - H_i) \cdot (e_{i+1} - e_i) - 100 \cdot e_{i+1}}.$$

Set $h = h' - 360$ if $h' > 360$, otherwise $h = h'$.

Step 2: Calculate t, e_t, p_1, p_2 and p_3

$$t = \left[\frac{C}{\sqrt{\frac{J}{100}} \cdot (1.64 - 0.29^n)^{0.73}}\right]^{\frac{1}{0.9}},$$

$$e_t = \frac{1}{4} \cdot \left[\cos\left(h \cdot \frac{\pi}{180} + 2\right) + 3.8\right],$$

$$A = A_w \cdot \left(\frac{J}{100}\right)^{\frac{1}{c \cdot z}},$$

$$p_1 = \left(\frac{50000}{13} \cdot N_c \cdot N_{cb}\right) \cdot e_t \cdot \left(\frac{1}{t}\right), \quad \text{if } t \neq 0,$$

$$p_2 = \frac{A}{N_{bb}} + 0.305,$$

$$p_3 = \frac{21}{20},$$

Step 3: Calculate a and b

If $t = 0$, then $a = b = 0$ and go to Step 4

(be sure transferring h from degree to radian before calculating $\sin(h)$ and $\cos(h)$)

If $|\sin(h)| \geq |\cos(h)|$, then

$$p_4 = \frac{p_1}{\sin(h)},$$

$$b = \frac{p_2 \cdot (2 + p_3) \cdot \left(\frac{460}{1403}\right)}{p_4 + (2 + p_3) \cdot \left(\frac{220}{1403}\right) \cdot \left(\frac{\cos(h)}{\sin(h)}\right) - \left(\frac{27}{1403}\right) + p_3 \cdot \left(\frac{6300}{1403}\right)},$$

$$a = b \cdot \left(\frac{\cos(h)}{\sin(h)}\right).$$

If $|\cos(h)| > |\sin(h)|$, then

$$p_5 = \frac{p_1}{\cos(h)},$$

$$a = \frac{p_2 \cdot (2 + p_3) \cdot \left(\frac{460}{1403}\right)}{p_5 + (2 + p_3) \cdot \left(\frac{220}{1403}\right) - \left[\left(\frac{27}{1403}\right) - p_3 \cdot \left(\frac{6300}{1403}\right)\right] \cdot \left(\frac{\sin(h)}{\cos(h)}\right)},$$

$$b = a \cdot \left(\frac{\sin(h)}{\cos(h)}\right).$$

Step 4: Calculate R'_{a}, G'_{a} and B'_{a}

$$R'_{\mathrm{a}} = \frac{460}{1403} \cdot p_2 + \frac{451}{1403} \cdot a + \frac{288}{1403} \cdot b,$$

$$G'_{\mathrm{a}} = \frac{460}{1403} \cdot p_2 - \frac{891}{1403} \cdot a - \frac{261}{1403} \cdot b,$$

$$B'_{\mathrm{a}} = \frac{460}{1403} \cdot p_2 - \frac{220}{1403} \cdot a - \frac{6300}{1403} \cdot b.$$

Step 5: Calculate R', G' and B'

$$R' = \mathrm{sign}(R'_{\mathrm{a}} - 0.1) \cdot \frac{100}{F_L} \cdot \left[\frac{27.13 \cdot |R'_{\mathrm{a}} - 0.1|}{400 - |R'_{\mathrm{a}} - 0.1|}\right]^{\frac{1}{0.42}}.$$

Here, $\mathrm{sign}(x) = \begin{cases} 1 & \text{if } x > 0 \\ 0 & \text{if } x = 0 \\ -1 & \text{if } x < 0 \end{cases}$, and similarly computing G', and B' from G'_{a}, and B'_{a}.

Step 6: Calculate R_{C}, G_{C} and B_{C} (for the inverse matrix, see the note at the end of the Appendix)

$$\begin{pmatrix} R_{\mathrm{c}} \\ G_{\mathrm{c}} \\ B_{\mathrm{c}} \end{pmatrix} = M_{\mathrm{CAT02}} \cdot M_{\mathrm{HPE}}^{-1} \cdot \begin{pmatrix} R' \\ G' \\ B' \end{pmatrix}.$$

Step 7: Calculate R, G and B

$$\begin{pmatrix} R \\ G \\ B \end{pmatrix} = \begin{pmatrix} \frac{R_{\mathrm{c}}}{D_{\mathrm{R}}} \\ \frac{G_{\mathrm{c}}}{D_{\mathrm{G}}} \\ \frac{B_{\mathrm{c}}}{D_{\mathrm{B}}} \end{pmatrix}.$$

Step 8: Calculate X, Y and Z (for the coefficients of the inverse matrix, see the note
at the end of the Appendix)

$$\begin{pmatrix} X \\ Y \\ Z \end{pmatrix} = M_{\mathrm{CAT02}}^{-1} \cdot \begin{pmatrix} R \\ G \\ B \end{pmatrix}.$$

Notes to Appendix

1. It is recommended to use the matrix coefficients given below for the inverse
matrix M_{CAT02}^{-1} and M_{HPE}^{-1}:

$$M_{\mathrm{CAT02}}^{-1} = \begin{pmatrix} 1.096124 & -0.278869 & 0.182745 \\ 0.454369 & 0.473533 & 0.072098 \\ -0.009628 & -0.005698 & 1.015326 \end{pmatrix},$$

$$M_{\mathrm{HPE}}^{-1} = \begin{pmatrix} 1.910197 & -1.112124 & 0.201908 \\ 0.370950 & 0.629054 & -0.000008 \\ 0.000000 & 0.000000 & 1.000000 \end{pmatrix}$$

2. For implementing the CIECAM02, the testing data and the corresponding results
from the forward and reverse modes can be found from reference 7.
3. The L_{A} is computed using (2.11)

$$L_{\mathrm{A}} = \left(\frac{E_{\mathrm{W}}}{\pi} \right) \cdot \left(\frac{Y_{\mathrm{b}}}{Y_{\mathrm{W}}} \right) = \frac{L_{\mathrm{W}} \cdot Y_{\mathrm{b}}}{Y_{\mathrm{W}}}, \tag{2.11}$$

where $E_{\mathrm{w}} = \pi \cdot L_{\mathrm{w}}$ is the illuminance of reference white in lux unit; L_{w} the luminance
of reference white in cd/m^2 unit, Y_{b} the luminance factor of the background and Y_{w}
the luminance factor of the reference white.

References

1. Luo MR (1999) Colour science: past, present and future. In: MacDonald LW and Luo MR
(Eds) Colour imaging: vision and technology. Wiley, New York, 384–404
2. CIE Technical Report (2004) Colorimetry, 3rd ed. Publication 15:2004, CIE Central Bureau,
Vienna.

3. Luo MR, Cui GH, Rigg B (2001) The development of the CIE 2000 colour difference formula. Color Res Appl 26:340-350.
4. Luo MR, Hunt RWG (1998) The structure of the CIE 1997 colour appearance model (CIECAM97s). Color Res Appl 23:138–146
5. CIE (1998) The CIE 1997 interim colour appearance model (simple version), CIECAM97s. CIE Publication 131, CIE Central Bureau, Vienna, Austria.
6. Moroney N, Fairchild MD, Hunt RWG, Li C, Luo MR, Newman T (2002) The CIECAM02 color appearance model, Proceedings of the 10th color imaging conference, IS&T and SID, Scottsdale, Arizona, 23–27
7. CIE (2004) A colour appearance model for colour management systems: CIECAM02, CIE Publication 159 CIE Central Bureau, Vienna, Austria
8. Luo MR and Li CJ (2007) CIE colour appearance models and associated colour spaces, Chapter 11 of the book: colorimetry-understanding the CIE System. In: Schanda J (ed) Wiley, New York
9. Luo MR, Cui GH, Li CJ and Rigg B (2006) Uniform colour spaces based on CIECAM02 colour appearance model. Color Res Appl 31:320–330
10. Xiao K, Luo MR, Li C, Hong G (2010) Colour appearance prediction for room colours, Color Res Appl 35:284–293
11. Xiao K, Luo MR, Li CJ, Cui G, Park D (2011) Investigation of colour size effect for colour appearance assessment, Color Res Appl 36:201–209
12. Xiao K, Luo MR, Li CJ (2012) Color size effect modelling, Color Res Appl 37:4–12
13. Fu CY, Li CJ, Luo MR, Hunt RWG, Pointer MR (2007) Quantifying colour appearance for unrelated colour under photopic and mesopic vision, Proceedings of the 15th color imaging conference, IS&T and SID, Albuquerque, New Mexico, 319–324
14. Li CJ, Chorro-Calderon E, Luo MR, Pointer MR (2009) Recent progress with extensions to CIECAM02, Proceedings of the 17th color imaging conference, IS&T and SID, Albuquerque, New Mexico 69–74
15. CIE Publ. 17.4:1987, International lighting vocabulary, the 4th edition
16. Mori L, Sobagaki H, Komatsubara H, Ikeda K (1991) Field trials on CIE chromatic adaptation formula. Proceedings of the CIE 22nd session, 55–58
17. McCann JJ, McKee SP, Taylor TH (1976) Quantitative studies in Retinex theory: a comparison between theoretical predictions and observer responses to the 'color mondrian' experiments. Vision Res 16:445–458
18. Breneman EJ (1987) Corresponding chromaticities for different states of adaptation to complex visual fields. J Opt Soc Am A 4:1115–1129
19. Helson H, Judd DB, Warren MH (1952) Object-color changes from daylight to incandescent filament illumination. Illum Eng 47:221–233
20. Lam KM (1985) Metamerism and colour constancy. Ph.D. thesis, University of Bradford, UK
21. Braun KM, Fairchild MD (1996) Psychophysical generation of matching images for cross-media colour reproduction. Proceedings of 4th color imaging conference, IS&T, Springfield, Va., 214–220
22. Luo MR, Clarke AA, Rhodes PA, Schappo A, Scrivener SAR, Tait C (1991) Quantifying colour appearance. Part I. LUTCHI colour appearance data. Color Res Appl 16:166–180
23. Luo MR, Gao XW, Rhodes PA, Xin HJ, Clarke AA, Scrivener SAR (1993) Quantifying colour appearance, Part IV: transmissive media. Color Res Appl 18:191–209
24. Kuo WG, Luo MR, Bez HE (1995) Various chromatic adaptation transforms tested using new colour appearance data in textiles. Color Res Appl 20:313–327
25. Juan LY, Luo MR (2000) New magnitude estimation data for evaluating colour appearance models. Colour and Visual Scales 2000, NPL, 3-5 April, UK
26. Juan LY, Luo MR (2002) Magnitude estimation for scaling saturation. Proceedings of 9th session of the association internationale de la couleur (AIC Color 2001), Rochester, USA, (June 2001), Proceedings of SPIE 4421, 575–578
27. Li CJ, Luo MR, Rigg B, Hunt RWG (2002) CMC 2000 chromatic adaptation transform: CMCCAT2000. Color Res Appl 27:49–58

28. Judd DB (1940), Hue, saturation, and lightness of surface colors with chromatic illumination. J Opt Soc Am 30:2–32
29. Kries V (1902), Chromatic adaptation, Festschrift der Albrecht-Ludwig-Universitat (Fribourg), [Translation: MacAdam DL, Sources of Color Science, MIT Press, Cambridge, Mass. (1970)]
30. Luo MR, Hunt RWG (1998) A chromatic adaptation transform and a colour inconstancy index. Color Res Appl 23:154–158
31. Li CJ, Luo MR, Hunt RWG (2000) A revision of the CIECAM97s Model. Color Res Appl 25:260–266
32. Hunt RWG, Li CJ, Juan LY, Luo MR (2002), Further improvements to CIECAM97s. Color Res Appl 27:164–170
33. Finlayson GD, Süsstrunk S (2000) Performance of a chromatic adaptation transform based on spectral sharpening. Proceedings of IS&T/SID 8th color imaging conference, 49–55
34. Hunt RWG (1952) Light and dark adaptation and perception of color. J Opt Soc Am 42:190–199
35. Stevens JC, Stevens SS (1963) Brightness functions: effects of adaptation. J. Opt Soc Am 53:375–385
36. Bartleson CJ, Breneman EJ (1967) Brightness perception in complex fields. J. Opt Soc Am 57:953–957
37. Luo MR, Gao XW, Sciviner SAR (1995) Quantifying colour appearance, Part V, Simultaneous contrast. Color Res Appl 20:18–28
38. Wyszecki G, Stiles WS (1982) Color Science: concepts and methods, Quantitative data and formulae. Wiley, New York
39. Helson H (1938) Fundamental problems in color vision. I. The principle governing changes in hue, saturation, and lightness of non-selective samples in chromatic illumination. J Exp Psych 23:439–477
40. CIE Publ. 152:2003, Moroney N, Han Z (2003) Field trials of the CIECAM02 colour appearance, Proceedings of the 25th session of the CIE, San Diego D8-2–D8-5.
41. Tastl I, Bhachech M, Moroney N, Holm J (2005) ICC colour management and CIECAM02, Proceedings of the 13th of CIC, p 318
42. Gury R, Shaw M (2005) Dealing with imaginary color encodings in CIECAM02 in an ICC workflow. Proceedings of the 13th of CIC, pp 217–223
43. Li CJ, Luo MR, Cui GH (2003) Colour-difference evaluation using colour appearance models. The 11th Color Imaging Conference, IS&T and SID, Scottsdale, Arizona, November, 127–131
44. Luo MR, Rigg B (1986) Chromaticity–discrimination ellipses for surface colours. Color Res Appl 11:25–42
45. Berns RS, Alman DH, Reniff L, Snyder GD, Balonon-Rosen MR (1991) Visual determination of suprathreshold color-difference tolerances using probit analysis. Color Res Appl 16:297–316
46. Hunt RWG (1952) Measuring colour, 3rd edition, Fountain Press, Kingston-upon-Thames, 1998
47. Li CJ, Chorro-Calderon E, Luo MR, Pointer MR (2009) Recent progress with extensión to CIECAM02, Seventeenth Colour Imaging Conference, Final Program and Proceedings, 69–74
48. Brill MH (2006) Irregularity in CIECAM02 and its avoidance. Color Res Appl 31(2):142–145
49. Brill MH, Susstrunk S (2008) Repairing gamut problems in CIECAM02: a progress report. Color Res Appl 33(5):424–426
50. Süsstrunk S, Brill M (2006) The nesting instinct: repairing non nested gamuts in CIECAM02. 14th SID/IS&T color imaging conference
51. Li CJ, Perales E, Luo MR, Martínez-Verdú F, A Mathematical approach for predicting non-negative tristimulus values using the CAT02 chromatic adaptation transform, Color Res Appl (in press)
52. ISO 15076-1 (2005) Image technology, colour management-Architecture, profile format and data structure-Part I: based on ICC.1:2004-10, http://www.color.org
53. Moroney N (2003) A hypothesis regarding the poor blue constancy of CIELAB. Color Res Appl 28(5):371–378

54. W. Gill GW (2008) A solution to CIECAM02 numerical and range issues, Proceedings of the 16th of color imaging conference, IS&T and SID, Portland, Oregan 322–327

55. Kuo CH, Zeise E, Lai D (2006) Robust CIECAM02 implementation and numerical experiment within an ICC workflow. Proceedings of the 14th of CIC, pp 215–219

56. Hunt RWG, Li CJ, Luo MR (2002) Dynamic cone response functions for modes of colour appearance. Color Res Appl 28:82–88

57. Paula J, Alessi P (2008) Private communication pursuit of scales corresponding to equal perceptual brightness, personal correspondence